rt Anno 2010_Numero 171

rapporti tecnici INGV

# Comparison between Different Heat Source Functions in Thermal Conduction Problems

171

Istituto Nazionale di Geofisica e Vulcanologia

**Direttore**
Enzo Boschi

**Editorial Board**
Raffaele Azzaro (CT)
Sara Barsotti (PI)
Mario Castellano (NA)
Viviana Castelli (BO)
Rosa Anna Corsaro (CT)
Luigi Cucci (RM1)
Mauro Di Vito (NA)
Marcello Liotta (PA)
Simona Masina (BO)
Mario Mattia (CT)
Nicola Pagliuca (RM1)
Umberto Sciacca (RM1)
Salvatore Stramondo (CNT)
Andrea Tertulliani - Editor in Chief (RM1)
Aldo Winkler (RM2)
Gaetano Zonno (MI)

**Segreteria di Redazione**
Francesca Di Stefano - coordinatore
Tel. +39 06 51860068
Fax +39 06 36915617
Rossella Celi
Tel. +39 06 51860055
Fax +39 06 36915617

redazionecen@ingv.it

Anno 2010_Numero 171

rapporti tecnici INGV

# COMPARISON BETWEEN DIFFERENT HEAT SOURCE FUNCTIONS IN THERMAL CONDUCTION PROBLEMS

Andrea Bizzarri

**INGV** (Istituto Nazionale di Geofisica e Vulcanologia, Sezione di Bologna)

171

## Table of contents

## Introduction

The problem of heat conduction in solids has become very attractive in the recent years, because there is an increasing consensus on the prominent role played by the temperature evolution in the physics of earthquake ruptures. As summarized by Bizzarri (2010a), the temperature field due to frictional heating on a frictional interface (the fault surface) can activate different, and potentially competing, chemical and physical mechanisms.

These processes can strongly modify the traction evolution (and the subsequent seismic waves excitation) with respect to "classical" (let say standard or canonical) fault models where all these second–order effects were a priori neglected. Far from being exhaustive, we simply mention here the thermal pressurization of fluids [Andrews, 2002; Bizzarri and Cocco, 2006], the flash heating of micro–asperity contacts [e.g., Noda et al., 2009] and the melting of rocks [Nielsen et al., 2008].

Basically, in the literature two different heat source functions have been introduced in order to solve the Fourier's heat conduction equation; the first one has been introduced by Fialko (2004) and by Bizzarri and Cocco (2006) and the second one is due to Andrews (2002). Each of these two heat sources gives an analytical solution for the temperature field, but a systematic (and quantitative) comparison of these expressions is actually missed. The main aim of the present study is to fill this gap.

## 1. Statement of the problem

The fault geometry considered in this study is the same as that described in details in Bizzarri (2010b); the fault is planar, vertical and strike slip and it is defined by the plane $x_2 = x_2^f$. The surrounding medium is perfectly elastic and $x_3 = 0$ is the free surface (where the tractions–free boundary condition is applied).

On the fault a constitutive equation [see Bizzarri, 2010a for a review] is prescribed to describe the deviation of this interface from the elasticity of the surrounding medium. The fundamental elasto–dynamic equation is solved numerically as in Bizzarri and Cocco (2005).

We will also consider a fault structure as indicated by geological inferences [see Chester and Chester, 1998, among many others], where the slip is concentrated in a slipping zone of width $2w$, which is surrounded by a highly fractured damage zone, where elasto–plastic processes are expected to take place (Figure 1a). For sake of simplicity we adopt the simple model reported in Figure 1b, where the slipping zone thickness is assumed to have a constant width, independently on the strike and dip coordinates ($\xi_1$ and $\xi_3$, respectively) and homogeneous properties. Moreover, the size of the slipping zone is constant through time; this assumption is quite reasonable within the cosesimic time scale we consider, although these time variations can be relevant in the whole seismic cycle of the fault (Bizzarri, 2010d). The local coordinate $\zeta$ indicates the distance from the center of the slipping zone ($x_2 = x_2^f$) which we associate to the mathematical plane representing the fault.

In the remainder of the study we will denote with $v$ and $\tau$ the magnitude (i.e., the $\ell^2$–norm) of the fault slip velocity and traction vectors, respectively. These quantities are formally defined in the center of the slipping zone mentioned above, which represents the mathematical fault plane. Moreover, we do not presently have sufficient information in order to model the behavior of the damage zone surrounding the fault.

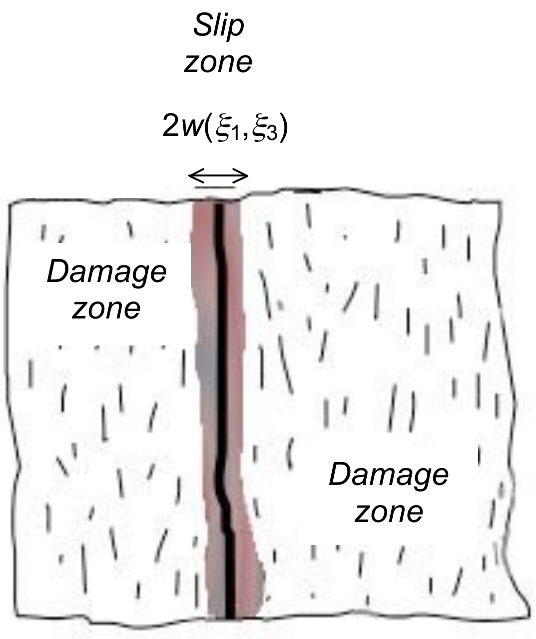


**(a)**

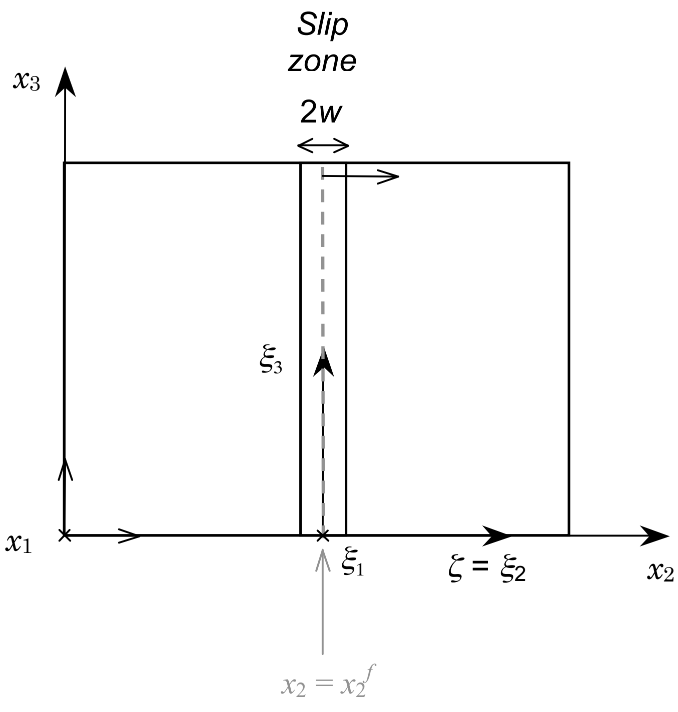


**(b)**

**Figure 1.** Schematic representation of the fault structure considered in the present study. (a) Sketch showing the coupling between the slipping zone, where deformations are concentrated, and the surrounding damage zone. (b) Mathematical simplification of the model, consisting in homogeneous and planar slipping zone.

Let we now consider the 1–D Fourier's heat conduction equation, which reads:

$$\frac{\partial}{\partial t} T(\zeta, t) = \chi \frac{\partial^2}{\partial \zeta^2} T(\zeta, t) + \frac{1}{c} q(\zeta, t) \tag{1}$$

where $t$ is the time, $T$ is the temperature field, $\chi$ is the thermal diffusivity, $c$ is the heat capacity of the bulk composite for unit volume, and $q$ is the heat source. The PDE in equation (1) can be solved once the heat source function is defined. In the next two sections we will analyze the two cases proposed in the literature. As in Bizzarri (2010b) we will consider the cosesimic time window, discretized through time steps of the order of milliseconds or less.

## 2. Heat source within a finite thickness

By considering an elementary heat source which is instantaneous and point–like in space,

$$q^{el}(\zeta,t) = h\ \delta(\zeta)\ \delta(t), \tag{2}$$

where $[h]$ = J/m$^2$ is the intensity of the source and $\delta(.)$ is the Dirac's delta, it is possible to find the following analytical solution for the elementary heat conduction problem (i.e., the problem arising from equation (1) with $q = q^{el}$):

$$T^{el}(\zeta, t) = \frac{h}{2c\sqrt{\pi \chi t}} \mathrm{e}^{-\frac{\zeta^2}{4\chi t}} \tag{3}$$

To solve equation (1) in the general case of heat produced by frictional heating on a sliding interface, in agreement with Fialko (2004), Bizzarri and Cocco (2006) consider the following heat source:

$$q(\zeta, t) = \begin{cases} \dfrac{\tau(t) v(t)}{2w} & , t > 0, |\zeta| \le w \\ 0 & , |\zeta| > w \end{cases} \tag{4}$$

The solution of problem (1) is therefore expressed as the convolution in time between the Green's kernel (3) and the actual heat source (4), integrated over the whole $\zeta$–domain:

$$\begin{aligned} T(\zeta, t) &= T(\zeta, 0) + \frac{1}{2c\sqrt{\pi\chi}} \int_0^t \mathrm{d}t' \int_{-\infty}^{+\infty} \mathrm{d}\zeta' \frac{1}{\sqrt{t - t'}} \mathrm{e}^{-\frac{(\zeta - \zeta')^2}{4\chi(t - t')}} q(\zeta', t') \\ &= T(\zeta, 0) + \frac{1}{2cw\sqrt{\pi\chi}} \int_0^t \mathrm{d}t' \int_{-w}^{+w} \mathrm{d}\zeta' \frac{\tau(t') v(t')}{\sqrt{t - t'}} \mathrm{e}^{-\frac{(\zeta - \zeta')^2}{4\chi(t - t')}} \end{aligned} \tag{5}$$

Now, since it holds:

$$\lim_{t' \to t^-} \frac{\mathrm{e}^{-\frac{1}{t - t'}}}{\sqrt{t - t'}} = 0 \tag{6}$$

we have that it is possible to truncate the calculation of the time integral in equation (5) up to the time $t - \varepsilon$, being $\varepsilon$ an arbitrarily small, positive, real number. In conclusion, we can write the solution of equation (1) in the limit of $\zeta \to 0$ (i.e., on the fault plane) as [Bizzarri and Cocco, 2006; Appendix A] as follows:

$$T^{(B)}(t) = T_0 + \frac{1}{2cw} \int_0^{t-\varepsilon} \mathrm{d}t' \ \mathrm{erf}\left( \frac{w}{2\sqrt{\chi(t-t')}} \right) \tau(t')v(t') \tag{7}$$

in which $T_0$ is the initial temperature on the fault plane (i.e., $T(\zeta = 0, t = 0)$) and erf(.) is the error function ( $\mathrm{erf}(z) \underset{\mathrm{df}}{=} \frac{2}{\sqrt{\pi}} \int_0^z \mathrm{d}x \, \mathrm{e}^{-x^2}$ ).

## 3. Gaussian–shaped heat source

Andrews (2002) solves the elementary heat conduction problem by considering the following elementary heat source function:

$$q^{el}(\zeta, t) = \frac{h}{\sqrt{2\pi}\, w} \mathrm{e}^{-\frac{\zeta^2}{2w^2}} \delta(t) \tag{8}$$

with again $[h] = \mathrm{J/m^2}$. Taking into account equation (8) it is possible to obtain the elementary solution of (1):

$$T^{el}(\zeta, t) = \frac{h}{c\sqrt{\pi}\sqrt{4\chi t + 2w^2}} \mathrm{e}^{-\frac{\zeta^2}{4\chi t + 2w^2}} \tag{9}$$

Now, to solve the general problem (1) Andrews (2002) considers the actual heat source as follows (the intensity $h\delta(t)$ in (8) is replaced by $v(t)\tau(t)$):

$$q(\zeta, t) = \frac{\tau(t)v(t)}{\sqrt{2\pi}\, w} \mathrm{e}^{-\frac{\zeta^2}{2w^2}} \tag{10}$$

which physically represents the fact that the 68 % of the (non elastic) deformation occurs within a thickness of size $2w$. The general solution of equation (1) coupled with (10) is then:

$$T(\zeta, t) = T_0 + \frac{1}{c\sqrt{\pi}} \int_0^t \mathrm{d}t' \frac{\tau(t')v(t')}{\sqrt{4\chi(t-t') + 2w^2}} \mathrm{e}^{-\frac{\zeta^2}{4\chi(t-t') + 2w^2}} \tag{11}$$

In particular, in the limit of $\zeta \to 0$ we have:

$$T^{(A)}(t) = T_0 + \frac{1}{c\sqrt{\pi}} \int_0^t \mathrm{d}t' \frac{\tau(t')v(t')}{\sqrt{4\chi(t-t') + 2w^2}} \tag{12}$$

## 4. Comparison of the different solutions I: Analytical details

First of all we note that both the heat source functions (4) and (10) contain an explicit dependence on the length scale characterizing the fault structure ($w$).

An important difference between the solution pertaining to a source within a thin layer (equation (7)) and that pertaining to a Gaussian source (equation (12)) is that that the former depends on the time histories of velocity and traction up to the previous time instant, while the latter exhibits a clear coupling between $T^{(A)}$, $v$ and $\tau$. This has important implications from a numerical point of view, because the fault traction $\tau$ can depend on the temperature and therefore the three quantities $T^{(A)}$, $v$ and $\tau$ have to be determined simultaneously. In fact, $\tau$ can depend explicitly on the temperature, as in the governing model inferred from laboratory experiments by Chester and Higgs (1992; see also Bizzarri, 2010c). On the other hand $\tau$ can depend on $T$ implicitly, when thermal pressurization of pore fluids is considered and a temperature–dependent time variation of effective normal stress affects the value of $\tau$ [see Bizzarri and Cocco, 2006 for further analytical details].

On the contrary, in the first case $T^{(B)}$ can be easily computed at time $t$ since at that time $v$ and $\tau$ enter in the calculation up to the previous time instant $t - \varepsilon$.

An interesting result emerges by calculating the limit of the two solutions (7) and (12) in the case of vanishing thickness of the slipping zone; when $w \to 0$ both the solutions converge to the same expression:

$$T(t) = T_0 + \frac{1}{2c\sqrt{\pi\chi}} \int_0^{t-\varepsilon} \mathrm{d}t' \, \frac{1}{\sqrt{t-t'}} \tau(t') v(t') \tag{13}$$

because it holds:

$$\lim_{w \to 0} \frac{\operatorname{erf}\left(\frac{w}{K}\right)}{w} = \frac{2}{K\sqrt{\pi}} \tag{14}$$

where in our case $K \equiv 2\sqrt{\chi(t-t')}$. (Note that in this limit case, the integration of the solution pertaining to the Gaussian source has been also truncated at the time instant $t - \varepsilon$ in that it does not converge for $t = t'$.) We also emphasize that both actual heat sources (equations (4) and (10)) pertaining to the two different models gives the same heat flux $\Phi$ (with $[\Phi] = \mathrm{W/m^2}$); by integrating equations (4) and (10) over the coordinate $\zeta$ we obtain the same heat produced per unit fault area and per unit time:

$$\Phi(t) = \tau(t)\, v(t). \tag{15}$$

Interestingly, equation (13) is the classical solution [e.g., McKenzie and Brune, 1972] that pertains to a heat source concentrated only in a fault of null thickness, which has been already considered in a previous study [Bizzarri, 2010b].

## 5. Comparison of the different solutions II: Numerical tests

In order to have a quantitative estimate of the differences existing between the different time histories of temperatures obtained assuming the two different heat sources discussed above, we have to numerically compare them. We assume the same thermal parameters as in Bizzarri and Cocco (2006) and we perform the numerical comparison in a target fault point.

We also assume the time histories of fault slip velocity $v$ and fault traction $\tau$ and we then compute the resulting $T^{(B)}$ and $T^{(A)}$ as in equations (7) and (12), respectively. The selected time histories of $v$ and $\tau$ are the same used in Bizzarri (2010b), reported in Figure 2 for convenience. We emphasize here that the assumed time history of the traction is representative of fault nodes located not so close to the free surface, where we recall the traction–free condition is applied (see section 1).

The results of the numerical comparison is reported in Figure 3. We have explored the parameter space of the slipping zone thickness $2w$, by assuming the typical values suggested by geological and experimental observations.

We can clearly see that by assuming a Gaussian–shaped heat source (equation (10) the resulting temperature is generally lower than that pertaining to the heat source defined within a thin layer (equation (4)); in other words, we have that $T^{(A)} < T^{(B)}$.

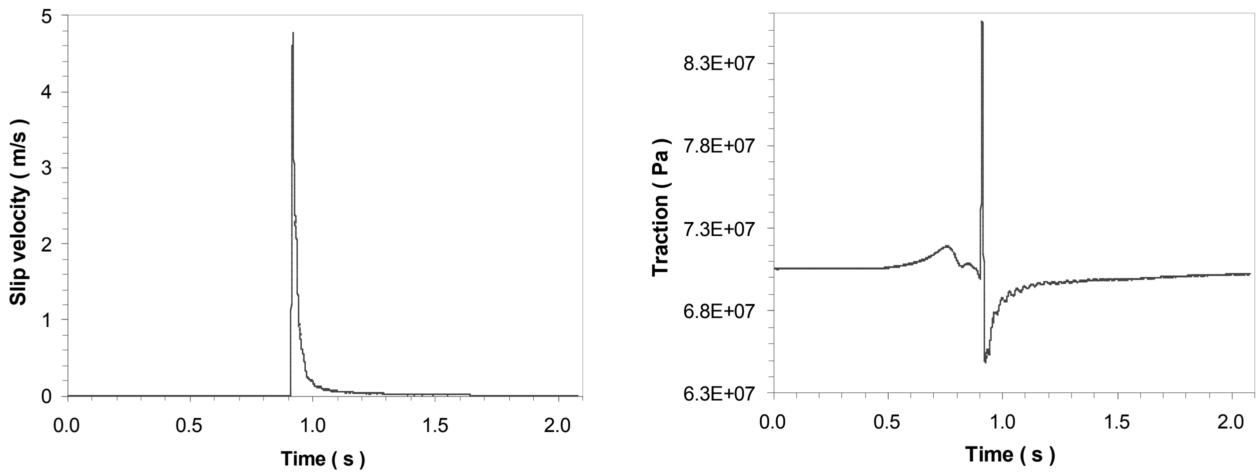


**(a)** **(b)**

**Figure 2.** Time histories of the fault slip velocity $v$ (panel (a)) and traction $\tau$ (panel (b)) adopted in the computation of the temperature fields pertaining to the two different heat sources considered in the present study. We use the same time histories as in Bizzarri (2010b).

It is also interesting to emphasize that when $w$ = 1 mm the evolution of $T^{(B)}$ is such that melting is expected to occur (in that the melting temperature $T_{melt}$ — which is estimated between 1100 °C and 1550 °C; Di Toro Pennacchioni, 2004 — is exceeded), while $T^{(B)}$ remains below $T_{melt}$.

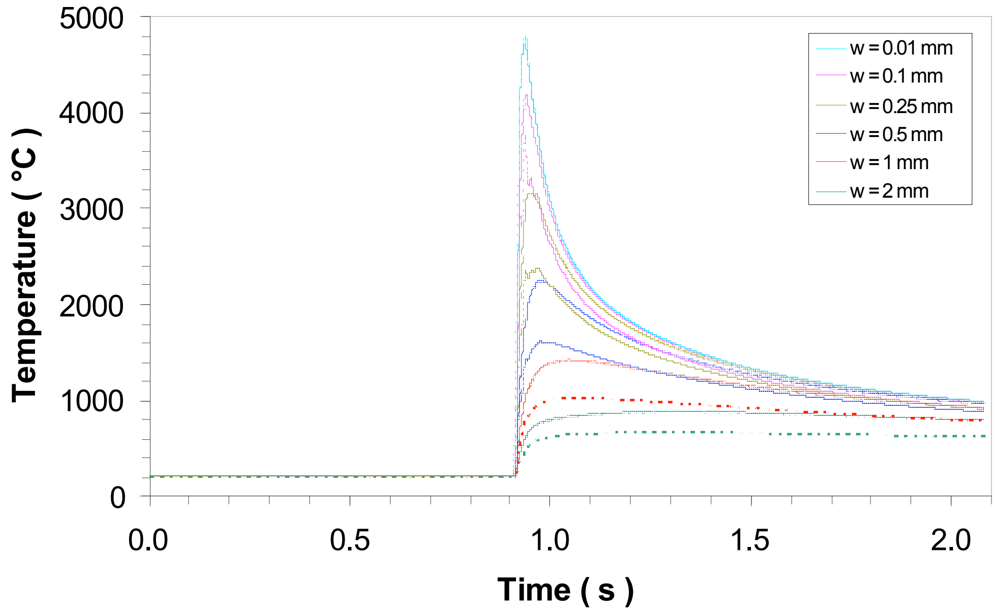


**Figure 3.** Comparison between the temperatures histories pertaining to the heat source in a finite thickness ($T^{(B)}$ as in equation (7); solid curves) and those pertaining to the Gaussian heat source ($T^{(A)}$ as in equation (12); dashed curves). The different values of the slipping zone thickness are reported in the legend.

In Figure 4 we report the percent misfit between the two solutions $T^{(B)}$ and $T^{(A)}$. Namely, we plot the non dimensional quantity

$$M = 100 \frac{T^{(B)} - T^{(A)}}{T^{(B)}}. \tag{16}$$

From Figure 4 it emerges that the differences between the two solutions tend to be more pronounced as far as the slipping zone thickness increases. Notably, for $w \leq 0.01$ mm $T^{(B)}$ and $T^{(A)}$ are quite similar and the only differences correspond to the breakdown process, corresponding to the peak in fault slip velocity and to the stress release. This is not surprising, since we have already noticed that the two expressions converge to the same result (equation (13)) in the limit of $w \to 0$.

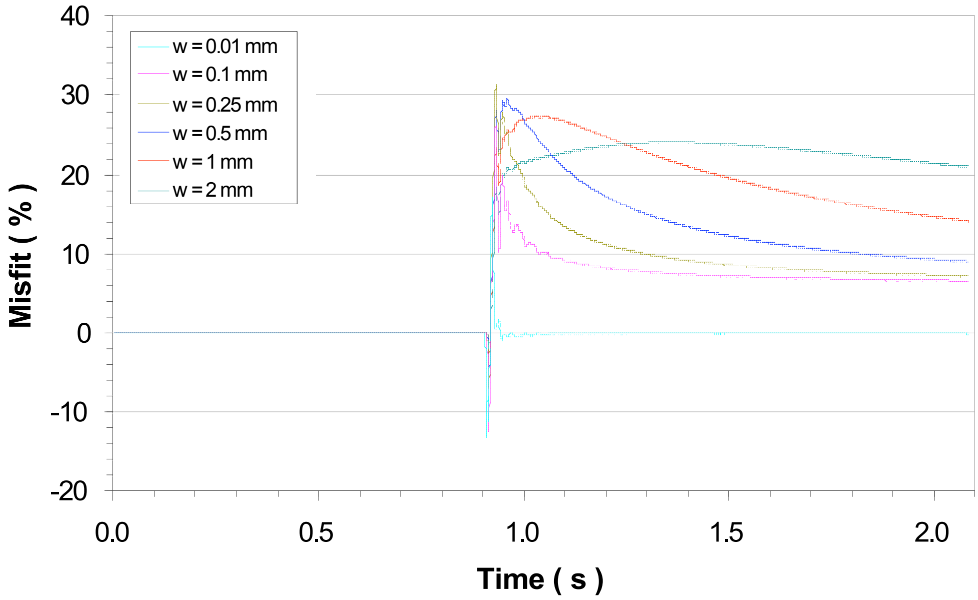


**Figure 4.** Misfit between the two temperature histories reported in Figure 3. The misfit reported in ordinate axis is define in equation (16).

## 6. Summary

The temperature due to frictional heating is an important ingredient in the attempts to describe, as much realistically is possible, the chemical and physical processes occurring in crustal faulting.

The conductive problems relying on the Fourier's equation can be solved analytically for point sources and for special cases of heat sources $q$. When actual heat source have more complicated expression the solution can be accomplished thought the convolution between a Green's kernel (the solution of an elementary problem) and the actual expression of $q$.

In this study we have compared to rather different approaches; the first one has been adopted by Fialko (2004) in 2–D and by Bizzarri and Cocco (2006) in 3–D numerical simulations and the second one has been introduced by Andrews (2002) in 3–D. The former approach assumes a heat source defined in a finite layer (section 2), while the latter defines a Gaussian–shaped heat source (section 3). Correspondently, the two temperature evolutions are different in the two cases. We summarize the analytical expression in Table 1.

The numerical comparison (Figures 3 and 4) shows that the analytical expressions, for a given set of parameters and for assigned time histories of fault slip velocity and traction, lead to a different prediction in terms of temperature evolution.

In general, the Gaussian–shaped heat source function tends to produce lower temperatures than those predicted by the other heat source. Moreover, we have found that the differences are more pronounces as far as the slipping zone thickness increases (Figure 4); this is not surprising, since we have shown that the two solutions converge to the same analytical expression when $w \rightarrow 0$ (see equation (13)).

| *Type of heat source* | ***Thin layer (section 2)*** | ***Gaussian–shaped (section 3)*** |
|---|---|---|
| *Elementary heat source* | $q^{el}(\zeta,t) = h\ \delta(\zeta)\ \delta(t)$ | $\mathrm{q}^{\mathrm{el}}(\zeta,\mathrm{t}) = \dfrac{\mathrm{h}}{\sqrt{2\pi}\ \mathrm{w}}\ \mathrm{e}^{-\frac{\zeta^2}{2\mathrm{w}^2}}\ \delta(\mathrm{t})$ |
| *Elementary solution of equation (1)* | $T^{el}(\zeta,t) = \dfrac{h}{2c\sqrt{\pi\chi t}}\ \mathrm{e}^{-\frac{\zeta^2}{4\chi t}}$ | $T^{el}(\zeta,t) = \dfrac{h}{c\sqrt{\pi}\ \sqrt{4\chi t + 2w^2}}\ \mathrm{e}^{-\frac{\zeta^2}{4\chi t + 2w^2}}$ |
| *Actual heat source* | $q(\zeta,t) = \begin{cases} \dfrac{\tau(t)v(t)}{2w} & , t > 0, \lvert\zeta\rvert \le w \\ 0 & , \lvert\zeta\rvert > w \end{cases}$ | $q(\zeta,t) = \dfrac{\tau(t)v(t)}{\sqrt{2\pi}\ w}\ \mathrm{e}^{-\frac{\zeta^2}{2w^2}}$ |
| *Solution of equation (1) in the general case* | $T^{(B)}(t) = T_0 + \dfrac{1}{2cw}\displaystyle\int_0^{t-\varepsilon} \mathrm{d}t'\ \mathrm{erf}\left(\dfrac{w}{2\sqrt{\chi(t-t')}}\right)\ \tau(t')v(t')$ | |
| | | $T^{(A)}(t) = T_0 + \dfrac{1}{c\sqrt{\pi}}\displaystyle\int_0^{t} \mathrm{d}t' \dfrac{\tau(t')v(t')}{\sqrt{4\chi(t-t') + 2w^2}}$ |

**Table 1.** Synoptic comparison of the two approaches for the solution of the conductive problem (equation (1)) considered in the present work.

To finish, the present study clearly demonstrates that the choice of the heat source function introduced to solve the 1–D heat conduction DPE can change the obtained analytical solution. In particular our numerical computations show that, even for relatively small thicknesses of the slipping zone ($w > 0.01$ mm), the resulting temperature evolution is therefore affected by the choice of the actual heat source function.

## Acknowledgements

I whish to acknowledge Gaetano Festa for his fruitful comments that contributed to clarify some aspects of the present work.

## References

Andrews, D. J. (2002). A fault constitutive relation accounting for thermal pressurization of pore fluid, J. Geophys. Res., 107, No. B12, 2363, doi: 10.1029/2002JB001942.

Bizzarri, A. (2010a). Toward the formulation of a realistic fault governing law in dynamic models of earthquake ruptures, in *Dynamic Modelling*, Edited by Alisson V. Brito, INTECH, Vienna, ISBN 978-953-7619-68-8, 167–188, http://www.sciyo.com/articles/show/title/toward-the-formulation-of-a-realistic-fault-governing-law-in-dynamic-models-of-earthquake-ruptures.

Bizzarri, A. (2010b). Determination of the temperature field due to frictional heating on a sliding interface, Rapporti Tecnici I.N.G.V., 158, 1–16.

Bizzarri, A. (2010c). Pulse‐like dynamic earthquake rupture propagation under rate–, state– and temperature–dependent friction, Geophys. Res. Lett., 37, L18307, doi: 10.1029/2010GL044541.

Bizzarri, A. (2010d). On the recurrence of earthquakes: Role of wear in brittle faulting, Geophys. Res. Lett., 37, L20315, doi: 10.1029/2010GL045480.

Bizzarri, A., Cocco, M. (2005). 3D dynamic simulations of spontaneous rupture propagation governed by different constitutive laws with rake rotation allowed. Ann. Geophysics, 48, No. 2, 279–299.

Bizzarri, A., Cocco, M. (2006). A thermal pressurization model for the spontaneous dynamic rupture propagation on a three–dimensional fault: 1. Methodological approach, J. Geophys. Res., 111, B05303, doi: 10.1029/2005JB003862.

Chester, F. M., Chester J. S. (1998). Ultracataclasite structure and friction processes of the Punchbowl fault, San Andreas system, California, Tectonophys., 295, 199–221.

Chester, F. M., Higgs, N. G. (1992). Multimechanism friction constitutive model for ultrafine gouge at hypocentral conditions, J. Geophys. Res., 97, 1859–1870, doi: 10.1029/91JB02349.

Di Toro, G., Pennacchioni, G. (2004). Superheated friction–induced melts in zoned pseudotachylytes within the Adamello tonalities (Italian southern Alps), J. Struct. Geol., 26, 1783–1801.

Fialko, Y. A. (2004). Temperature fields generated by the elastodynamic propagation of shear cracks in the Earth, J. Geophys. Res., 109, No. B01303, doi: 10.1029/2003JB002497, 1–14.

McKenzie, D., Brune, J. N. (1972). Melting on fault planes during large earthquakes, Geophys. J. R. astr. Soc., 29, 65–78.

Nielsen, S., Di Toro, G., Hirose, T., Shimamoto, T. (2008), Frictional melt and seismic slip, J. Geophys. Res., 113, B01308, doi: 10.1029/2007JB005122.

Noda, H., Dunham, E. M., Rice, J. R. (2009). Earthquake ruptures with thermal weakening and the operation of major faults at low overall stress levels, J. Geophys. Res., 114, B07302, doi: 10.1029/2008JB006143.

Sibson, R. H. (2003), Thickness of the seismic slip zone, Bull. Seism. Soc. Am., 93, No. 3, 1169–1178.

**Coordinamento editoriale e impaginazione**
Centro Editoriale Nazionale | INGV

**Progetto grafico e redazionale**
Laboratorio Grafica e Immagini | INGV Roma

© 2010 INGV Istituto Nazionale di Geofisica e Vulcanologia
Via di Vigna Murata, 605
00143 Roma
Tel. +39 06518601 Fax +39 065041181

**http://www.ingv.it**

Istituto Nazionale di Geofisica e Vulcanologia